Available Online: 27 April 2026 DOI: 10.54254/2977-3903/2026.32980

Study on the low-temperature SCR performance of MnO_x/Cu-SSZ-13 composite catalyst

Haokai Ma

Lingnan University, Hong Kong, China

haokaima@ln.hk

Abstract. Due to the poor selling performance of Cu-SSZ-13 at low temperatures, better methods are needed for improvement. This article prepared MnO_x/Cu-SSZ-13 catalyst through impregnation method and physical mixing method. It was found that after activity testing, the MnO_x/Cu-SSZ-13 catalyst prepared by impregnation method showed the most significant improvement in Selective Catalytic Reduction (SCR) activity, with a NO_x conversion rate of 100% at 275℃. Moreover, the negative impact of the impregnation method on the high-temperature SCR activity of MnO_x/Cu-SSZ-13 catalyst was smaller than that of the physical mixing method. Through characterization analysis, it was found that the MnO_x crystals in the MnO_x/Cu-SSZ-13 catalysts prepared by impregnation and physical mixing methods have the same form. However, in the impregnation method samples, MnO_x is uniformly distributed on the surface of Cu-SSZ-13 with smaller particles, while in the physical mixing method, MnO_x is dispersed around Cu-SSZ-13 in a larger agglomerated form. Moreover, due to the large oxygen vacancies in the impregnation sample, there is a large amount of adsorbed oxygen, significantly improving the catalyst's ability to oxidize NO, resulting in a stronger interaction between Cu-SSZ-13 and MnO_x, accelerating electron transfer between Cu and Mn, and excellent oxidation ability. Therefore, the MnO_x/Cu-SSZ-13 catalyst prepared by impregnation method has better catalytic performance. Finally, by studying the SCR mechanism of composite catalysts, the structure-activity relationship between MnO_x and Cu-SSZ-13 on NH3-SCR performance was established, providing a theoretical basis for the development of composite catalysts.

Keywords: SCR, Cu-SSZ-13, composite catalyst, impregnation method

1. Introduction

1.1. Research background

1.1.1. Sources of NO_x

Nitrogen Oxides (NO_x) are a class of harmful atmospheric pollutants. Their primary sources include the following: emissions from combustion processes, natural sources, and agricultural activities.

According to the 2022 *China Mobile Source Environmental Management Annual Report,* with the rapid rise of new energy vehicles in China over the past two years, their number has increased by nearly 2.17 million compared with the previous year. However, vehicles emitting NO_x exhaust still account for more than

80% of the total, exhibiting the characteristic of relatively small individual scale but disproportionately large pollution contributions [1, 2].

1.1.2. Hazards of NO_x

Nitrogen Oxides (NO_x) are among the most common atmospheric pollutants and are widely regarded as major contributors to air pollution. They pose significant risks to both human health and the environment:

1. Impacts on human health: NO_x can adversely affect the respiratory system, causing symptoms such as shortness of breath, chest tightness, and chronic bronchitis.

2. Impacts on the environment: They are key components of smog, reducing visibility and degrading urban landscapes.

3. Impacts on the Earth system: Emissions of NO_x can damage the atmospheric environment, contributing to climate change, acid rain, and ozone layer depletion, thereby posing broader ecological threats.

Therefore, effective measures must be taken to reduce NO_x emissions. These include controlling emissions from industry and transportation, reducing nitrogen fertilizer use in agriculture, and promoting more sustainable personal travel behaviors.

1.2. NO_x control technologies

At present, NO_x control technologies can be broadly classified into three categories. The first is pre-combustion treatment, which involves reducing the nitrogen content in fuels or directly removing nitrogen compounds prior to combustion. The second is in-combustion control, which reduces NO_x formation by optimizing combustion conditions and improving combustion equipment. The third is post-combustion treatment, which primarily involves injecting reducing agents into flue gas and, with the aid of catalysts, selectively reducing NO to N_2, thereby achieving NO_x removal [3].

Although pre-combustion technologies exhibit high efficiency in NO_x control, their high cost and technical complexity limit their practical application. In contrast, combustion control technologies are widely used due to their lower cost, but their NO_x removal efficiency is relatively limited. When such methods fail to meet emission standards, post-combustion treatment technologies are required, which can be divided into wet denitrification and dry denitrification.

1.2.1. Wet denitrification technology

Wet flue gas denitrification is a method that removes nitrogen oxides through liquid-phase absorption. It operates based on two mechanisms: oxidation and reduction. In practice, the oxidation absorption method is most commonly used. In this process, oxidizing agents react with NO, converting insoluble NO into more soluble NO_2, which is subsequently absorbed by the solution. According to the reduction principle, reducing agents can also be added to convert NO_x into N_2 for direct removal [4].

1.2.2. Dry denitrification technology

Dry denitrification technologies include adsorption methods, plasma methods, thermal decomposition, Selective Non-Catalytic Reduction (SNCR), and Selective Catalytic Reduction (SCR).

(1) Adsorption Method: This method features a simple process, low operating cost, and no secondary pollution. However, it also suffers from drawbacks such as high adsorbent consumption, bulky equipment, and a tendency for pipeline blockage. As a result, its large-scale application remains limited [5, 6].

(2) Plasma Method: The plasma method [7] can simultaneously achieve desulfurization and denitrification. Nevertheless, due to its complex equipment, high energy consumption, and substantial investment cost, its practical application is constrained [8].

(3) Selective Non-Catalytic Reduction (SNCR): SNCR denitrification offers advantages such as simple operation, low capital investment, no requirement for catalysts, and minimal impact on boiler operation.

However, it also exhibits limitations, including relatively low NO_x removal efficiency, high operating temperature requirements, and significant ammonia slip. Consequently, SNCR has gradually been replaced by other denitrification technologies in practical applications.

(4) Selective Catalytic Reduction (SCR): The fundamental principle of SCR is the use of ammonia (NH_3) as a reducing agent to convert NO_x into N_2. The basic SCR process involves uniformly injecting NH_3 into flue gas at temperatures of 320–400 °C. The mixture then passes through a reactor packed with catalysts, where NO_x reacts with NH_3 under catalytic conditions according to the following reactions:

$$4NO + 4NH_3 + O_2 = 4N_2 + 6H_2O \quad (1)$$

$$8NH_3 + 6NO_2 = 7N_2 + 12H_2O \quad (2)$$

SCR technology is characterized by high NO_x removal efficiency (up to 80%–90%), low secondary pollution, technological maturity, and widespread application. However, it also involves relatively high capital and operating costs.

1.3. Current status of NH_3-SCR catalysts

The catalyst is the core component of SCR denitrification technology. At present, NH_3-SCR catalysts can be broadly classified into three categories: noble metal catalysts, molecular sieve catalysts, and metal oxide catalysts.

1.3.1. Noble metal catalysts

Noble metal catalysts use precious metals such as Pt, Rh, Pd, and Ru as active components [9]. These metals are typically supported on carriers such as Al_2O_3 [10], TiO_2 [11], and ZSM-5 [12]. Although noble metal catalysts exhibit excellent catalytic performance, their high cost and limited availability significantly restrict their large-scale application.

1.3.2. Molecular sieve catalysts

Molecular sieves can be classified according to pore size into microporous (< 2 nm), mesoporous (2–50 nm), and macroporous (> 50 nm) materials. Hierarchical molecular sieves combine the advantages of micropores and mesopores, offering broad application prospects in petrochemical processes and being widely studied in NH_3-SCR catalysis [13].

The pore structure, Si/Al ratio, and properties of exchanged metal ions in molecular sieves all have a significant influence on NO_x removal performance. Common zeolite materials include ZSM-5 [14], Beta [15], and SSZ-13 [16]. Copper-based molecular sieve catalysts exhibit excellent resistance to poisoning and high stability. Studies by KawK et al. [15] and Colombo et al. [16] have demonstrated that Cu-SSZ-13 shows superior catalytic performance compared with similar catalysts.

Optimizing the performance of Cu-SSZ-13 has become a major research focus. Zhang [17] introduced MnO_2–CeO_2 to enhance its low-temperature activity and sulfur resistance. Song Chaoming et al. [18] found that increasing the Mn/Cu ratio improves low-temperature activity. Chen Jiawei et al. [19] confirmed that increasing Cu content broadens the low-temperature activity window and enhances low-temperature performance, while having little effect on high-temperature performance.

1.3.3. Metal oxide catalysts

Metal oxide-based SCR catalysts constitute the most diverse and widely applied class of catalysts, among which Mn-based and V-based catalysts have attracted particular attention due to their excellent catalytic performance. Depending on whether a support is used, metal oxide catalysts can be divided into supported and unsupported types.

(1) CeO_2-Based CatalystsCeO_2-based catalysts possess high oxygen storage/release capacity and excellent redox properties. However, their relatively weak surface acidity results in poor catalytic activity when pure CeO_2 is used.

(2) MnO_x-Based CatalystsResearch both domestically and internationally has primarily focused on MnO_x catalysts. Mn-based metal oxide catalysts exhibit outstanding low-temperature SCR activity and thus hold great application potential. Tang et al. prepared β-MnO_2 and α-Mn_2O_3 via a redox hydrothermal method and investigated NH_3-assisted NO reduction at 150 °C. Catalytic evaluation showed that, compared with α-Mn_2O_3, β-MnO_2 achieved higher NO conversion, a higher N_2O formation rate, and a nearly identical N_2 formation rate per unit surface area. Therefore, β-MnO_2 exhibits higher N_2O selectivity in SCR reactions than α-Mn_2O_3. Compared with highly crystalline Mn oxides, amorphous catalysts prepared via solid-state reactions and co-precipitation methods display higher catalytic activity. Studies indicate that amorphous MnxOy facilitates proton transfer, allowing both surface and bulk atoms of the catalyst to participate in redox reactions, thereby enhancing SCR activity [20, 21].

Mn-based catalysts demonstrate excellent performance in low-temperature denitrification and thus show strong application prospects. Manganese oxides possess abundant acidic active sites and reactive surface oxygen species. Their half-filled d orbitals facilitate electron transfer to O_2 and NH_3, promoting the selective reduction of NO_x. MnO_x-based catalysts, characterized by high specific surface area, abundant amorphous phases, and multiple valence states (MnO_2 > Mn_5O_8 > Mn_2O_3 > Mn_3O_4 > MnO), exhibit excellent denitrification performance at low temperatures [22]. However, single-component MnO_x catalysts suffer from poor resistance to water vapor and SO_2, as well as relatively low N_2 selectivity, which severely limits their industrial application [23]. To address these issues, researchers have introduced promoters such as CeO_2 to form composite MnO_x catalysts. This modification effectively enhances specific surface area and resistance to poisoning, thereby improving overall catalytic performance [24-27].

1.4. Research origin, content, and technical route

1.4.1. Research origin

Selective Catalytic Reduction (SCR) is currently the mainstream technology for controlling NO_x emissions. Among various approaches, NH_3-SCR—using NH_3 as the reducing agent—has been widely applied in mobile source denitrification. Since catalysts are the core of SCR technology, the development of highly efficient and stable SCR catalysts is of urgent importance. The SCR activity of Cu-SSZ-13 catalysts largely depends on the chemical state of copper. However, at low temperatures, the oxidation half-cycle from Cu^+ to Cu^{2+} is inhibited, preventing effective NO activation. As a result, Cu-SSZ-13 exhibits relatively poor denitrification activity under low-temperature conditions.

1.4.2. Research content

The main objectives of this study include the following: preparing MnO_x/Cu-SSZ-13 catalysts via physical mixing and impregnation methods; evaluating and comparing their SCR performance; employing multiple characterization techniques to analyze the influence of oxide structures on surface species of Cu-SSZ-13; clarifying the critical role of active oxygen in the formation of nitrate intermediates; and elucidating the low-temperature SCR reaction mechanisms of MnO_x/Cu-SSZ-13 composite catalysts prepared by the two methods.

1.4.3. Technical route

The technical route of this study is shown in Figure 1.

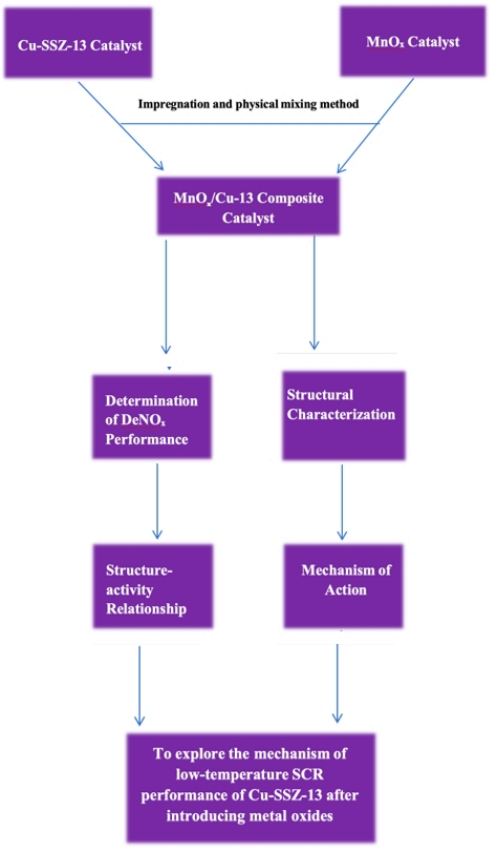

Figure 1. Technical route

2. Experimental methods and materials

2.1. Experimental materials and instruments

The raw materials and equipment used in this study are listed in Table 1.

Table 1. Materials and instruments for experiments

Category	Name
Chemical reagents	Anhydrous copper sulfate, deionized water, NH_4-SSZ-13, nitric acid, ammonium bicarbonate, quartz sand, manganese nitrate tetrahydrate
Cylinder gases	NH_3/N_2, N_2, O_2, NO/N_2
Instruments and equipment	Tablet press, oil-free air compressor, multi-position magnetic heating stirrer, electric thermostatic blast drying oven, standard test sieve, high-temperature muffle furnace, electronic balance

2.2. Catalyst preparation

2.2.1. Cu-SSZ-13 catalyst

(1) Prepare a copper sulfate solution. (2) Add NH_4-SSZ-13 to the copper sulfate solution. (3) Conduct ion exchange of Cu^{2+}.

2.2.2. MnO_x/cu-13 composite catalyst

The catalysts were prepared mainly by the impregnation method and the physical mixing method.

Impregnation method: A manganese nitrate solution was prepared and impregnated onto the Cu-SSZ-13 support using the incipient wetness impregnation method. After drying and calcination, the MnO_x/Cu-13 composite catalyst was obtained.

Physical mixing method: Ammonium carbonate was used as a precipitating agent. $Mn(NO_3)_2 \cdot 4H_2O$ was added, and the pH was adjusted to 8 using ammonia solution. After washing, filtration, and drying, the precipitate was calcined to obtain MnO_x. The resulting MnO_x was then mixed with Cu-SSZ-13 in a certain proportion, followed by grinding, tableting, and sieving (40–60 mesh) to obtain the composite catalyst.

2.3. Catalyst evaluation setup and procedure

2.3.1. Catalyst evaluation setup

The system consists of a gas distribution system, gas mixer, flue gas preheater, reactor, flue gas analysis system, and flue gas purification system.

2.3.2. Catalyst activity test

(1) A simulated flue gas mixture containing controlled concentrations of NO, NH_3, N_2, and O_2 was prepared using the gas distribution system, and baseline data were recorded. (2) MnO_x/Cu-13 composite catalysts prepared by different methods were crushed, pressed into pellets, and tested. NO_x removal efficiency curves were plotted to evaluate the influence of preparation methods on catalyst activity.

The concentrations of NO and NO_2 were recorded, and the NO_x conversion was calculated according to Equation (3).

$$NO_x \text{ Conversion} = \frac{(NO_x)_{\text{inlet}} - (NO_x)_{\text{outlet}}}{(NO_x)_{\text{inlet}}} \times 100\% \quad (3)$$

2.4. Catalyst characterization methods

2.4.1. Inductively Coupled Plasma (ICP) analysis

ICP analysis atomizes the sample under high temperature in an inert atmosphere, enabling complete evaporation, atomization, ionization, and excitation. The emitted characteristic spectral lines of elements are then detected. This technique is used to determine the content of active components in the catalyst.

2.4.2. X-ray diffraction (XRD) analysis

X-ray Diffraction (XRD) was used to analyze the phase composition, crystal structure, and crystal planes of the materials, and to compare crystallinity changes before and after reaction. The scanning range was 10–80° (2θ), with a step size of 0.02° and a scanning rate of $2° \cdot min^{-1}$, yielding diffraction patterns of the samples.

2.4.3. H_2 Temperature-Programmed Reduction (H_2-TPR)

The redox properties of the catalysts were investigated using H_2-TPR. Prior to testing, samples were pretreated at 200 °C in He (30 $mL \cdot min^{-1}$) for 1 h. The TPR measurements were conducted from room temperature to 900 °C under a flow of 10 vol% H_2/He (50 $mL \cdot min^{-1}$) with a heating rate of 10 $°C \cdot min^{-1}$.

2.4.4. Transmission Electron Microscopy (TEM) analysis

A Hitachi Regulus 8100 instrument (Japan) was used to obtain Scanning Electron Microscopy (SEM) and elemental mapping images of the samples, allowing observation of their dispersion characteristics.

2.4.5. Electron Paramagnetic Resonance (EPR) analysis

Electron Paramagnetic Resonance (EPR) is used for both qualitative and quantitative detection of unpaired electrons in atoms or molecules, and for probing their local structural environment.

2.4.6. X-ray Photoelectron Spectroscopy (XPS)

XPS measurements were carried out using an AXIS ULTRA DLD instrument (Kratos, UK) with an Al Kα radiation source. The binding energies of all elements were calibrated using the C 1s peak at 284.6 eV. Data analysis was performed using XPSPEAK software, with all binding energies referenced to the C 1s peak at 284.6 eV.

2.4.7. NO_x temperature-programmed desorption (NO_x-tpd)

NO_x-TPD was conducted using a BELCat II analyzer (Microtrac, Japan). The desorbed gases were monitored by a mass spectrometer, and the spectra were recorded. The monitored species and their corresponding mass-to-charge ratios (m/z) were NO (30) and NO_2 (46).

2.4.8. In situ Fourier Transform Infrared spectroscopy (FTIR)

In situ FTIR measurements were performed on a Nicolet iS50 spectrometer (Thermo Fisher Scientific, USA) equipped with a high-temperature reaction cell fitted with ZnSe windows and a liquid nitrogen-cooled MCT detector. DRIFTS measurements were conducted at 200 °C. The background spectrum was collected after purging the catalyst with N_2, followed by introduction of the target gases for analysis.

3. Catalyst activity and characterization analysis

3.1. Activity evaluation of Cu-SSZ-13 catalysts prepared by different methods

Figure 2 presents the denitrification performance of MnO_x/Cu-SSZ-13 catalysts prepared by different methods. Both composite catalysts exhibit favorable low-temperature SCR activity.

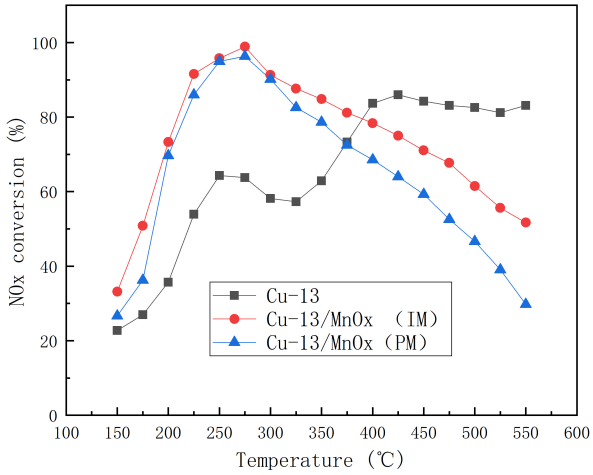

Figure 2. NO_x conversion of MnO_x/Cu-13 catalysts with different preparation methods

At 150 °C, the NO_x conversion of Cu-SSZ-13 is slightly above 20%, while the conversion rates of MnO_x/Cu-13 prepared by the impregnation and physical mixing methods are 33% and 27%, respectively. With increasing temperature, the conversion gradually rises, exceeding 90% for both catalysts at 250 °C. Among them, the impregnation-prepared sample shows higher efficiency, reaching 100% conversion at 275 °C, whereas the maximum conversion of undoped Cu-SSZ-13 is only 64%.

As the temperature increases further, the NO_x conversion of both composite catalysts declines continuously, and the second activity peak observed for Cu-SSZ-13 at 375–425 °C does not appear. At 550 °C, the conversion rates of the impregnation and physical mixing samples decrease to 51% and 30%, respectively.

In summary, the incorporation of MnO_x significantly enhances the low-temperature SCR activity of Cu-SSZ-13 but suppresses its high-temperature activity. Comparatively, the MnO_x/Cu-13 catalyst prepared by the impregnation method exhibits the most pronounced improvement in low-temperature activity, with minimal adverse impact on high-temperature performance.

3.2. Characterization analysis

3.2.1. Inductively Coupled Plasma (ICP) analysis

The ICP results are shown in Table 2. The Cu content in MnO_x/Cu-13 catalysts prepared by the three methods is consistent with the nominal values. After mixing MnO_x at a ratio of 1:2, Mn is detected in the composite catalysts, with its content corresponding proportionally to that in MnO_x.

Table 2. , Inductively Coupled Plasma Spectroscopy (ICP) results table

Sample	Element	Content
1. Cu-SSZ-13	Cu	1.2088%
2. MnO_x/Cu-13 (Impregnation)	Cu	1.0565%
	Mn	7.2102%
3. MnO_x/Cu-13 (Physical Mixing)	Cu	1.1057%
	Mn	3.1550%

3.2.2. X-ray Diffraction (XRD) analysis

Figure 3 shows the XRD patterns of catalysts prepared by the two methods. To determine the structural characteristics of MnO_x in Cu-SSZ-13, XRD was employed to characterize the synthesized catalysts.

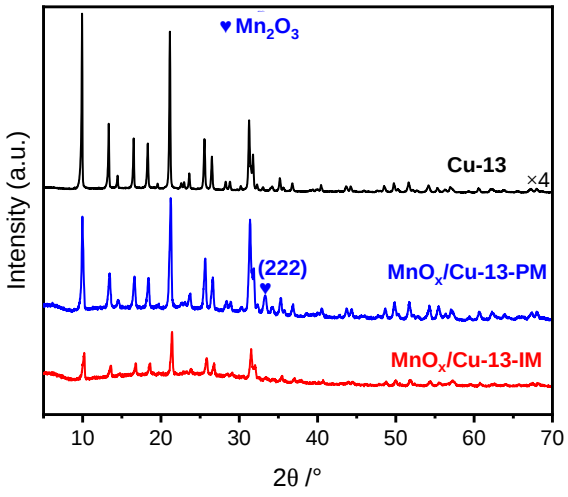

Figure 3. XRD patterns ofCu-SSZ-13, MnO_x/Cu-13-IM and MnO_x/Cu-13-PM

The Cu-SSZ-13 catalyst exhibits typical CHA-type diffraction peaks at 2θ = 9.5°, 14.0°, 16.1°, 17.8°, 20.7°, and 25.0°. After introducing MnO_x, the characteristic CHA diffraction peaks remain clearly observable [28, 29], indicating that neither the physical mixing nor the impregnation method alters the framework structure of Cu-SSZ-13. However, distinct differences are observed between the two preparation methods. The XRD pattern of the physically mixed sample shows characteristic diffraction peaks of Mn_2O_3 (2θ= 23°, 33°, 38°, 45°, and 55°; JCPDS: 71-0636), whereas no obvious MnO_x-related peaks are detected in the impregnated sample. This suggests that Mn species are more highly dispersed on the Cu-SSZ-13 support in the impregnated catalyst. To further clarify the structural features and dispersion of MnO_x, TEM characterization was conducted.

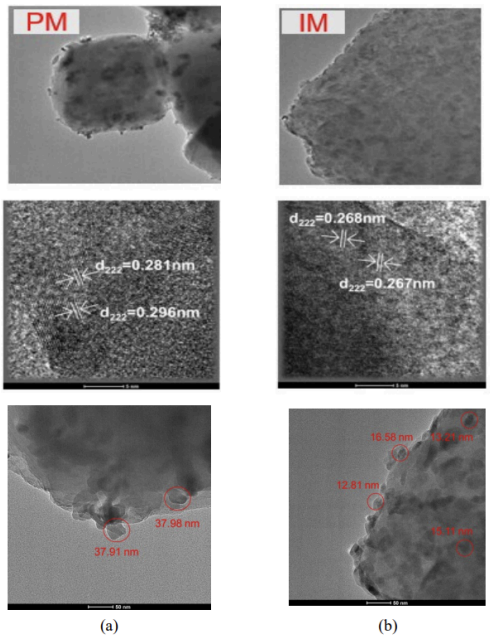

Figure 4. TEM image of Cu-SSZ-13, MnO_x/Cu-13-IM and MnO_x/Cu-13-PM.Therations are: (a) PM; (b) IM

3.2.3. Transmission Electron Microscopy (TEM) analysis

TEM analysis (Figure 4) reveals that Cu-SSZ-13 exhibits a typical cubic morphology, indicating successful synthesis of the SSZ-13 framework.

The introduction of MnO_x does not alter the morphology of the molecular sieve, consistent with the XRD results. Both the physically mixed and impregnated samples display lattice fringes with d-spacings of 0.267–0.296 nm. Based on XRD analysis and previous studies, these fringes can be attributed to the (222) crystal plane of Mn_2O_3. This indicates that MnO_x exists predominantly as Mn_2O_3 in both samples.

However, as shown in Figure 5, significant differences in dispersion are observed. In the physically mixed sample, MnO_x appears as irregular agglomerated particles with an average size of approximately 38 nm, distributed around the Cu-SSZ-13 support. In contrast, the impregnated sample exhibits uniformly dispersed MnO_x nanoparticles with sizes of 12–15 nm on the surface of Cu-SSZ-13. The smaller particle size and more uniform distribution facilitate better contact between reactants and active sites, which may account for the superior catalytic performance of the impregnated catalyst.

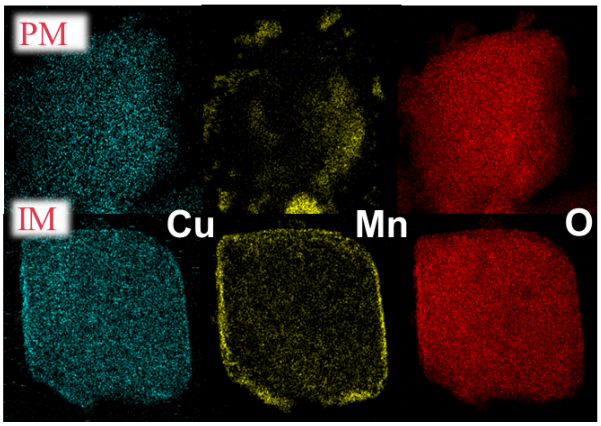

Figure 5. STEM-EDS elemental mappings over MnO_x/Cu-13-IM and MnO_x/Cu-13-PM

3.2.4. X-ray Photoelectron Spectroscopy (XPS) analysis

The XPS results (Figure 6) show that in the physically mixed sample, Mn^{3+}, Mn^{4+}, and Mn^{2+} account for 27%, 11%, and 62%, respectively. In contrast, the impregnated sample contains 55% Mn^{3+}, 21% Mn^{4+}, and 24% Mn^{2+}. Since Mn^{4+} promotes the oxidation of NO to NO_2 in low-temperature SCR reactions, the higher proportion of Mn^{4+} in the impregnated sample is beneficial for enhancing low-temperature activity.

In the O 1s spectra, the physically mixed sample contains 70% surface active oxygen (Oα) and 30% lattice oxygen (Oβ), whereas the impregnated sample contains 75% Oα and 25% Oβ. Surface active oxygen (Oα) has stronger oxidation capability; therefore, its higher proportion in the impregnated sample contributes to improved low-temperature denitrification performance.

Overall, the MnO_x/Cu-13 catalyst prepared by the impregnation method possesses a higher Mn^{4+} content and greater surface active oxygen concentration, both of which facilitate the low-temperature SCR reaction.

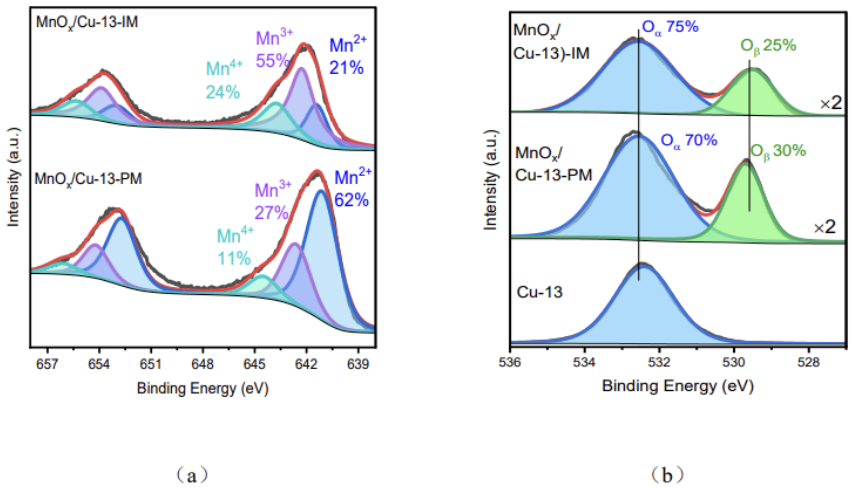

Figure 6. XPS spectra mappings over MnO_x/Cu-13-IM and MnO_x/Cu-13-PM

3.2.5. Electron Paramagnetic Resonance (EPR) analysis

EPR is an effective technique for detecting unpaired electrons in samples and can provide both qualitative and quantitative information on their local environments. The results are shown in Figure 7. Both samples exhibit an oxygen vacancy signal at g = 2.00. However, the EPR signal of MnO_x/Cu-13 (physical mixing) is weaker

than that of MnO_x/Cu-13 (impregnation), indicating that the impregnated sample contains a higher concentration of chemisorbed oxygen species. This enhances its redox capability, consistent with the XPS results. These findings further explain the superior low-temperature performance of the impregnated catalyst.

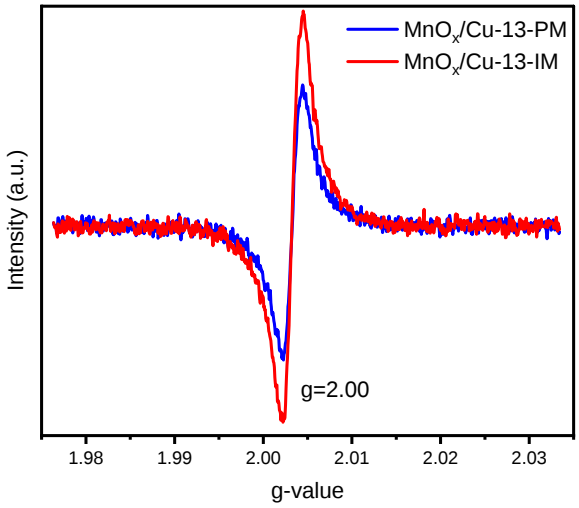

Figure 7. EPR patterns ofCu-SSZ-13,MnO_x/Cu-13-IM and MnO_x/Cu-13-PM

3.2.6. Redox properties: H_2-TPR analysis

The H_2-TPR profiles are shown in Figure 8. The Cu-SSZ-13 catalyst exhibits three reduction peaks at 217 °C, 420 °C, and 678 °C, corresponding to the reductions of $Cu^{2+}\rightarrow Cu^{+}$ in the eight-membered ring, $Cu^{2+}\rightarrow Cu^{+}$ in the six-membered ring, and $Cu^{+}\rightarrow Cu^{0}$, respectively.

The composite catalysts display four reduction peaks. For the impregnated sample, the peaks appear at 212 °C, 242 °C, and 325 °C, while for the physically mixed sample, they appear at 268 °C and 357 °C. The low-temperature peak at 212 °C is observed only in the impregnated sample and, combined with EPR and XPS results, is attributed to the reduction of adsorbed oxygen species. The peaks at 242 °C and 268 °C correspond to the reduction of Mn(III)→Mn(II), while those at 325 °C and 357 °C correspond to Mn(II)→Mn(0).

These results indicate that although MnO_x in both catalysts has similar crystal structures, its dispersion and chemical environment differ. The MnO_x/Cu-13 catalyst prepared by the impregnation method contains more oxygen vacancies, a higher concentration of chemisorbed oxygen, and higher Mn^{4+}/Mn and Oα/O ratios. These features enhance the interaction between MnO_x and Cu-SSZ-13, resulting in superior redox properties and improved low-temperature SCR performance compared with the physically mixed catalyst.

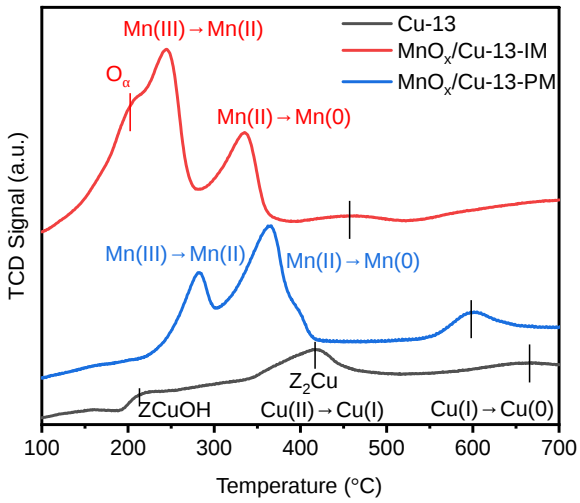

Figure 8. H_2-TPR patterns ofCu-SSZ-13,MnO_x/Cu-13-IM and MnO_x/Cu-13-PM

3.2.7. DRIFTS characterization analysis

In this section, in situ Diffuse Reflectance Infrared Fourier Transform Spectroscopy (DRIFTS) was employed to investigate the formation of intermediates during the adsorption of NO + O_2 over the binary catalysts MnO_x/Cu-13 and MC/Cu-13. The results are shown in Figure 9.

As illustrated in Figure 9, with the progression of NO adsorption at 200 °C, Cu-13 exhibits characteristic absorption bands at 1,625 cm^{-1}, 1,570 cm^{-1}, and 1,378 cm^{-1}. These peaks are attributed to nitrate intermediates formed via the activation of NO on Cu ionic sites. Specifically, the band at 1625 cm^{-1} corresponds to bridging nitrates, that at 1,570 cm^{-1} to bidentate nitrates, and that at 1,378 cm^{-1} to monodentate nitrates (1,592 cm^{-1}). Similarly, the DRIFTS spectra of the MnO_x/Cu-13 composite catalysts also display the same characteristic IR bands. Although DRIFTS confirms the formation and types of nitrate intermediates on all catalysts, quantitative analysis of nitrate species still requires NO_x-TPD characterization.

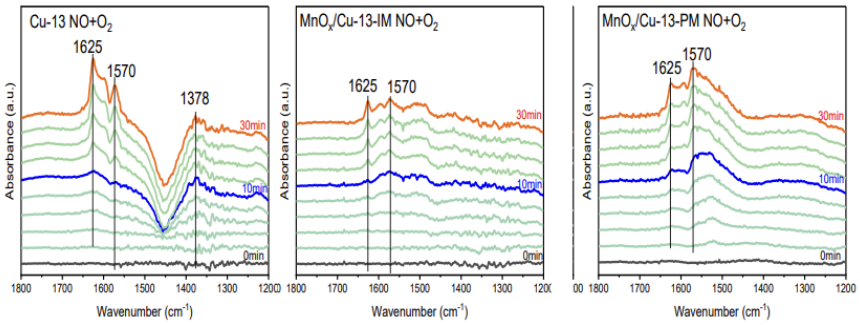

Figure 9. DRIFTS patterns of Cu-SSZ-13, MnO_x/Cu-13-IM and MnO_x/Cu-13-PM: (a) Cu-13; (b)MnO_x/Cu-13-IM; (c)MnO_x/Cu-13-PM

3.2.8. NO_x-TPD characterization analysis

NO_x-TPD measurements were conducted to quantitatively investigate the adsorption and activation behaviors of NO_x species on Cu-13 and the composite catalysts (Figure 10). No obvious desorption peaks are observed for the Cu-13 catalyst over the entire temperature range. For the physically mixed MnO_x/Cu-13 composite catalyst, only a small NO_x desorption peak appears. In contrast, the MnO_x/Cu-13 catalyst prepared via the impregnation method exhibits not only a small desorption peak but also a pronounced and broader NO_x desorption peak in the range of 300–400 °C. The amount of nitrate species on the MnO_x/Cu-13 catalyst prepared by impregnation is 32.9 mol/g, which is significantly higher than that of the physically mixed MnO_x/Cu-13 catalyst (0.59 mol/g).

Combined with the DRIFTS results, it can be concluded that similar types of nitrate intermediates are formed on the composite catalysts, but their quantities differ substantially. Therefore, the amount of nitrate intermediates is likely a critical factor in low-temperature SCR reactions.

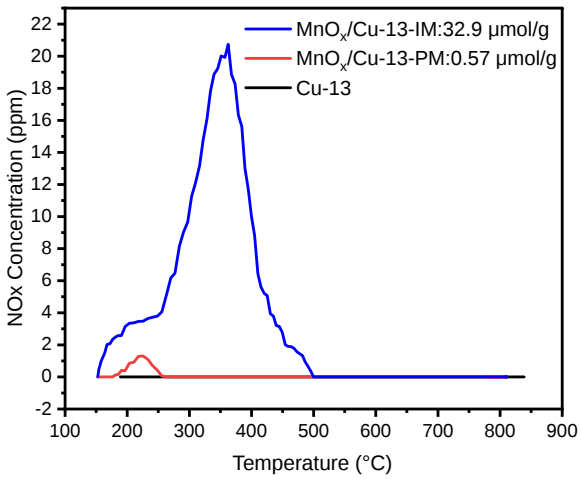

Figure 10. NO_x-TPD patterns ofCu-SSZ-13,MnO_x/Cu-13-IM and MnO_x/Cu-13-PM

3.2.9. Mechanistic study of low-temperature denitration over MnO_x/cu-ssz-13

Based on the above results, the MnO_x/Cu-13 composite catalyst prepared via the impregnation method exhibits superior low-temperature SCR performance. TEM results indicate that, in the impregnation-prepared catalyst, MnO_x is uniformly dispersed on the Cu-SSZ-13 surface as small crystallites (12–15 nm), whereas the physically mixed sample shows irregular agglomerated particles of approximately 38 nm. XPS and EPR analyses reveal that the impregnation-prepared catalyst possesses a higher concentration of oxygen vacancies, leading to increased chemisorbed oxygen species and Mn^{4+}, which are beneficial for accelerating the low-temperature SCR reaction. H_2-TPR further confirms the presence of strong interactions in the impregnation-prepared catalyst, promoting the electron transfer process ($Cu^{2+} + Mn^{3+} \rightarrow Cu^{+} + Mn^{4+}$) and endowing the catalyst with enhanced redox capability. NO_x-TPD and in situ DRIFTS results demonstrate that this catalyst exhibits stronger NO activation ability, generating a greater amount of nitrate intermediates, which subsequently react with NH_3 adsorbed on Cu-SSZ-13 to produce N_2 and H_2O. Therefore, the impregnation method is more effective for preparing high-performance MnO_x/Cu-SSZ-13 composite catalysts.

$$2NO + O_2 + 2O^* \rightarrow 2NO_3^{-*} \tag{4}$$

$$4NH_3 + 2NO_3^{-*} \rightarrow 3N_2 + 6H_2O \tag{5}$$

$$NO(g) \rightarrow NO(ad) \tag{6}$$

$$Mn^{4+} = O_{ads^-} + NO(ad) \rightarrow Mn^{4+} - NO_2^- \tag{7}$$

$$Mn^{4+} - NO_2^- + \tfrac{1}{2} O_2^- \rightarrow Mn^{3+} - NO_3^- \tag{8}$$

$$Mn^{3+} + \frac{1}{2} O_2^- \rightarrow Mn^{4+} = O_{ads^-} \tag{9}$$

4. Conclusions

4.1. Conclusions

By comparing the denitration performance of undoped and MnO_x-doped Cu-SSZ-13 catalysts, it was found that the introduction of MnO_x enhances the low-temperature SCR activity of Cu-SSZ-13, while slightly deteriorating its high-temperature performance. Catalytic activity tests indicate that the MnO_x/Cu-13 catalyst prepared via the impregnation method exhibits the most significant improvement in SCR performance, achieving 100% NO_x conversion at 275 °C, while showing the least negative impact on high-temperature activity.

Characterization results demonstrate that the framework structure of Cu-SSZ-13 remains unchanged regardless of the preparation method or MnO_x incorporation. Overall, the impregnation method is a more effective approach for synthesizing high-performance MnO_x/Cu-SSZ-13 composite catalysts.

4.2. Innovations

This study innovatively combines MnO_x with the Cu-SSZ-13 molecular sieve to construct a binary catalyst with excellent low-temperature denitration performance. Through comprehensive characterization techniques, the study systematically elucidates the role of reactive oxygen species in catalytic performance, as well as the redox cycle mechanism. Furthermore, the primary reasons and mechanistic pathways by which MnO_x promotes the low-temperature SCR activity of Cu-SSZ-13 are clearly identified.

4.3. Future perspectives

This study was conducted entirely under laboratory conditions. In practical applications, the atmospheric composition is far more complex; therefore, it is necessary to further evaluate the performance and stability of this catalytic system in the presence of multiple coexisting pollutants.

Although this work focuses on Mn-based metal oxides combined with Cu-SSZ-13, which are widely studied, it remains to be explored whether other metal oxides (such as Fe oxides and Co oxides) exhibit similar synergistic interactions. Further comparative investigations are required.

References

[1] He, H., Wang, Y., Ma, Q. X., Ma, J. Z., Chu, B., Ji, D. S., Tang, G. Q., Liu, C., Zhang, H. X., & Hao, J. (2014). Mineral dust and NO_x promote the conversion of SO_2 to sulfate in heavy pollution days. *Scientific Reports, 4*(1), 4172–4177.

[2] Paolucci, C., Khurana, I., & Parekh, A. (2017). Dynamic multinuclear sites formed by mobilized copper ions in NO_x selective catalytic reduction. *Science, 357*(6354), 898–903.

[3] Hao, J. M., Ma, G. D., & Wang, S. X. (2010). *Air pollution control engineering* (3rd ed., pp. 378–380). Beijing: Higher Education Press.

[4] Yang, J. Q., Mei, Y., Wang, C., Long, G. H., & Li, S. (2017). Current status and development of wet flue gas denitrification technology. *Chemical Industry and Engineering Progress, 36*(2), 695–704.

[5] Luo, S. L. (2017). Advantages, disadvantages, and development of activated carbon combined desulfurization and denitrification technology. *China Petroleum and Chemical Standards and Quality, 37*(24), 164–165.

[6] Wei, E. Z., Lin, H., Gao, X., Luo, Z. Y., Ni, M. J., & Cen, K. F. (2003). Plasma control technology for NO_x pollution in coal-fired boiler flue gas. *Techniques and Equipment for Environmental Pollution Control,* (1), 58–62.

[7] Meng, L. (2018). Current status and prospects of ion denitrification technology. *Science and Technology Information, 16*(3), 68–69.

[8] Liu, X. W., Li, J., Li, J. X., Ni, Z. X., Yi, X. L., & Lu, X. M. (2019). A review of flue gas denitrification technologies. *Guangzhou Chemical Industry, 47*(24), 53–55.

[9] Luca, L., Pio, F. I., Isabella, N., & Enrico, T. (2001). NO_x storage reduction over Pt–Ba/γ-Al_2O_3 catalyst. *Journal of Catalysis, 204*(1), 175–191.

[10] Zhang, Z., Chen, M., & Wang, S. G. (2009). Low-temperature SCR of NO with propylene in excess oxygen over Pt/TiO_2 catalyst. *Catalysis Communications, 10*(9), 1330–1333.

[11] Pérez-Ramírez, J., Jorge, M., García-Cortés, M. J. I., Freek, K., Jacob, A. M., & Salinas-Martínez, L. (2000). Reduction of NO by propene over Pt-, Pd-, and Rh-based ZSM-5 under lean-burn conditions. *Reaction Kinetics and Catalysis Letters, 69*(2), 385–392.

[12] Liu, N. N. (2019). *Theoretical study on the denitrification mechanism of Cu-SSZ-13 catalysts* [Doctoral dissertation, Hebei University of Technology].

[13] Long, R. Q., & Yang, R. T. (2000). Characterization of Fe-ZSM-5 catalyst for selective catalytic reduction of nitric oxide by ammonia. *Journal of Catalysis, 194*(1), 80–90.

[14] He, C. H., Wang, Y. H., & Cheng, Y. S. (2009). Stability and hydrocarbon deactivation of Fe/Beta catalyst for SCR of NO with ammonia. *Applied Catalysis A: General, 368*(1–2), 121–126.

[15] Kwak, J. H., Russell, G. T., Kim, D. H., Szanyi, J., & Peden, C. (2010). Excellent activity and selectivity of Cu-SSZ-13 in the selective catalytic reduction of NO_x with NH_3. *Journal of Catalysis, 275*(2), 187–190.

[16] Colombo, M., Koltsakis, G., Nova, I., & Tronconi, E. (2012). Modelling the ammonia adsorption–desorption process over an Fe zeolite catalyst for SCR automotive applications. *Catalysis Today, 188*(1), 42–52.

[17] Zhang, Y. N., Zhang, J., Wang, H. L., Yang, W. N., Wang, C. Z., Peng, Y., Chen, J. J., Li, J. H., & Gao, F. (2014). Selective catalytic reduction of NO_x with NH_3 over a Cu-SSZ-13 catalyst prepared by a solid-state ion-exchange method. *ChemCatChem, 6*(6), 1579–1583.

[18] Song, C. M. (2019). *Study on Mn-modified Cu-SSZ-13 catalysts and their NH_3-SCR performance* [Master's thesis, Tianjin University].

[19] Chen, J. W. (2019). *Synthesis and NH_3-SCR catalytic performance of metal-doped Cu-SSZ-13 molecular sieve catalysts* [Master's thesis, Zhejiang University].

[20] Zhu, L. (2018). *Study on denitrification performance and mechanism of low-temperature SCR catalysts based on transition metal oxides* [Doctoral dissertation, Southeast University].

[21] Tang, X., Li, J., Su, L., & Hao, J. (2010). Origination of N_2O from NO reduction by NH_3 over β-MnO_2 and α-Mn_2O_3. *Applied Catalysis B: Environmental*, 156–162.

[22] Jiang, B. (2008). *Preparation of Mn/TiO_2 low-temperature SCR DeNO_x catalysts and their reaction mechanism* [Doctoral dissertation, Zhejiang University].

[23] Yan, H., Zhang, N., & Wang, D. (2022). Highly efficient CeO_2-supported noble-metal catalysts: From single atoms to nanoclusters. *Chem Catalysis,* (1), 1594–1623.

[24] Tang, X., Hao, J., Xu, W., & Li, J. H. (2007). Low-temperature selective catalytic reduction of NO_x with NH_3 over amorphous MnO_x catalysts prepared by three methods. *Catalysis Communications, 8*(3), 329–334.

[25] Tian, W., Yang, H., Fan, X., & Zhang, X. B. (2011). Catalytic reduction of NO_x with NH_3 over different-shaped MnO_2 at low temperature. *Journal of Hazardous Materials, 188*(1), 105–109.

[26] Kapteijn, F., Vanlangeveld, A. D., Moulijn, J. A., Andreini, A., Vuurman, M. A., Turek, A. M., Jehng, J. M., & Wachs, I. E. (1994). Alumina-supported manganese oxide catalysts: I. Characterization—Effect of precursor and loading. *Journal of Catalysis, 150*(1), 94–104.

[27] Tang, X. L., Hao, J. M., Xu, W. G., & Li, J. H. (2006). Novel MnO_x catalysts for low-temperature NH_3-SCR of NO_x. *Chinese Journal of Catalysis,* (10), 843–848.

[28] Wang, Z. X. (2019). *Study on SO_2 sulfation and regeneration of Cu/SSZ-13 catalysts* [Master's thesis, Tianjin University].

[29] Zhou, S., Wang, H., Wang, S. N., & Liu, L. J. (2021). Effect of Si/Al ratio on the low-temperature catalytic performance of Cu/SSZ-13 molecular sieves. *Chemical Engineering, 49*(7), 61–66.